Model-simulated source contributions to PM2.5 in Santiago and the central region of Chile

(article starts on next page)

Model-simulated Source Contributions to PM$_{2.5}$ in Santiago and the Central Region of Chile

Joakim Langner[1*], Lars Gidhagen[1], Robert Bergström[1,2], Ernesto Gramsch[3], Pedro Oyola[4], Felipe Reyes[4], David Segersson[1], Claudio Aguilera[4]

[1] *Swedish Meteorological and Hydrological Institute, SE-60176 Norrköping, Sweden*
[2] *Department of Space, Earth and Environment, Chalmers University of Technology, SE-41296 Göteborg, Sweden*
[3] *University of Santiago de Chile, 9160000 Santiago, Chile*
[4] *Centro Mario Molina Chile, 7510121 Santiago, Chile*

ABSTRACT

The contributions to PM$_{2.5}$ from different emission sectors across central Chile and the Santiago metropolitan area during summer/fall and winter have been evaluated using a chemical transport model. The simulations generally underestimate the mean PM$_{2.5}$ concentrations compared to measurements conducted at stations in Santiago that belong to the Chilean National Air Quality Information System (SINCA). The potential reasons for this discrepancy include underestimated direct PM$_{2.5}$ emissions, missing emissions for semi- and intermediately volatile organic compounds (SVOCs and IVOCs) and overestimated wind speeds in the simulations. The simulated winter PM$_{2.5}$ concentrations in Santiago are lower and higher than the values observed during nighttime, and daytime and late evening, respectively, which may be related to excessive simulated wind speeds, as well as to uncertainties in the diurnal variation in the emissions. During summer/fall, the simulated diurnal variation better agrees with the observations, but the peak concentrations during the morning are underestimated, whereas those during the evening are overestimated. The simulated contributions of different aerosol components to the PM$_{2.5}$ at one station in Santiago are all lower than the observed values, except for elemental carbon equivalent black carbon (BC$_e$), which exhibit comparable or higher levels in the simulations. The absolute differences are the largest for the total organic matter, whereas the relative differences are the largest for BC$_e$ and ammonium. The simulated sector contributions indicate that emissions originating from transport and construction machinery dominate the PM$_{2.5}$ in Santiago; however, residential wood combustion is the primary source in other urban areas of central Chile, except near major point sources. Away from urban areas, traffic routes and major industrial sources, secondary inorganic aerosol (SIA) is estimated to be the largest component of the aerosol, whereas the simulated secondary organic aerosol (SOA) only contributes a small fraction.

Keywords: Secondary aerosol formation modeling; Urban; Chemical composition.

INTRODUCTION

Air pollution in Santiago de Chile (33.5°S, 70.8°W, 500 m a.s.l.) is a long-standing problem related to high anthropogenic emissions in the densely populated urban area and unfavorable geographical and meteorological settings. About 7 million inhabitants, a third of the Chilean population, lives in the Santiago metropolitan region (RM) and a large fraction of the Chilean industries are located there. Santiago is situated in a valley between the Andes mountain range (~5000 m a.s.l.) to the east and a coastal mountain range to the west (reaching about 1500 m a.s.l.). The climate is

Mediterranean, with hot and dry summers and more humid and cloudy winters. The region is under influence of the South Pacific subtropical anticyclone, which favors the generation of thermal inversions with low wind speeds. Low ventilation conditions are especially frequent during winter. Strong air pollution episodes are usually connected to specific synoptic settings including coastal lows and prefrontal conditions (Garreaud *et al.*, 2002). Particulate air pollution is a major concern, mainly due to negative impacts on human health (Grass and Dane, 2008; Cakmak *et al.*, 2009).

Chilean air quality standards for protection of human health and ecosystems were introduced in 1994. The metropolitan region has been declared a saturated zone (exceeding the standard) with regard to PM$_{10}$ since 1996 and a latent zone (concentrations in the range 80–100% of the standard) for SO$_2$ and ozone since 2010. For saturated zones atmospheric decontamination plans are developed to mitigate the problems and a plan for Santiago for PM$_{10}$ was put in place in 1997, with

---

subsequent updates, including multiple long-term efforts to reduce emissions. Consequently, concentrations of both PM_{10} and $PM_{2.5}$ have decreased in Santiago (Moreno *et al.*, 2010; Barraza *et al.*, 2017). In 2012 a national $PM_{2.5}$ standard was introduced. The standard for the annual mean concentration of $PM_{2.5}$ is 20 µg m^{-3} and for 24-h average, 50 µg m^{-3}. The standard also sets thresholds that are used to inform the public in connection with episodes. Despite efforts to reduce emissions, exceedances of the 24-h standard are frequently observed in wintertime in the Santiago metropolitan region.

Different aspects of the air quality situation in central Chile have been studied using regional chemical transport models (CTMs). These include studies of long-range transport of sulfur emissions from large copper smelters (Gallardo *et al.*, 2001; Olivares *et al.*, 2002) and dispersion of CO (Schmitz, 2005). Saide *et al.* (2016) developed a forecasting system for $PM_{2.5}$ in central and southern Chile, using a high resolution meteorological and chemistry forecast model for CO combined with observed correlations between CO and $PM_{2.5}$. Recently Mazzeo *et al.* (2018) studied the impact of direct emissions of $PM_{2.5}$ and NO_x, focusing on residential combustion and transport, during a 2-week episode in Santiago in 2015, using a regional CTM coupled to a high resolution meteorological model.

Successful policies for reducing PM pollution need to be based on a good understanding of major sources of air pollutants and their relative contributions to observed concentrations. In the present study we go several steps further compared to previous work and consider also the contribution from secondary aerosol formation, both organic and inorganic. We also examine contributions from the main emission sectors to concentrations of $PM_{2.5}$ for an extended period in summer/fall and winter 2012.

METHODS

Fig. 1 delineates the geographical domain considered. It encompasses an area of ca. 210×175 km^2 from the Pacific Ocean in the west to the Andes mountain range in the east, which are natural borders in terms of anthropogenic emissions. In the center of the domain lies the capital Santiago surrounded by the metropolitan region. To the south the domain includes the city of Rancagua and the northern parts of Region VI, and to the north and west the cities of San Felipe, Los Andes and Valparaiso/Viña del Mar in Region V. There are major industrial point sources located in Ventanas, on the coast in the northwestern part of the domain in Region V, and in Caletones, to the east of Rancagua in Region VI. There are also substantial emissions from mining activities in the Andes to the northeast of Santiago.

The time period studied is March–August 2012. This part of the year is dominated by the Southern Hemisphere winter which normally has the highest levels of particulate air pollution in the region, due to unfavorable meteorological conditions with low wind speeds and reduced vertical mixing. For this specific period a set of more extensive air quality measurements were available in Santiago, and the surrounding area, that could be used to evaluate model simulations.
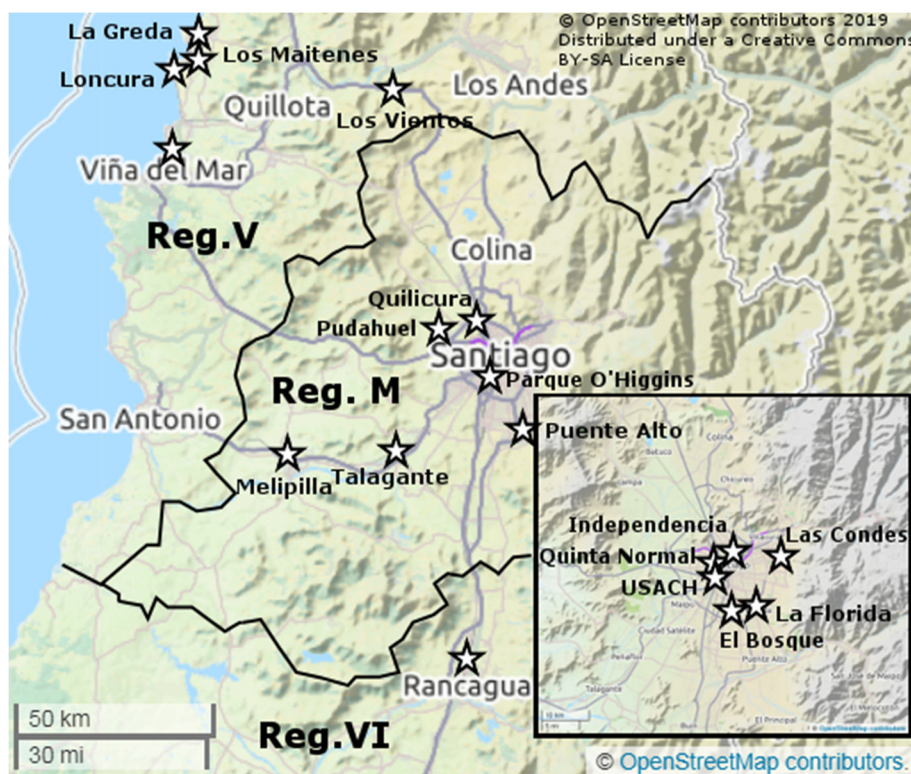

Fig. 1. Geographical domain with the locations of the different monitoring stations indicated. The inset shows the region surrounding Santiago in greater detail and also the area for which time variations in emissions are presented in Fig. 3. © OpenStreetMap contributors 2019. Distributed under a Creative Commons BY-SA License.

Observations

The locations of the monitoring sites in the domain are shown in Fig. 1. In order to evaluate the results of the model simulations, as much information as possible has been gathered for the simulated period (March–August 2012). Most stations used in this work belong to the Chilean National Air Quality Information System (SINCA) which measures at least the criteria pollutants, PM_{10}, $PM_{2.5}$, CO, NO_2, SO_2 and O_3, and meteorological parameters. Pollution data and detailed information about location, monitors used, etc., from these stations is available on the SINCA website (SINCA, 2018). The website has several filters that allow extracting data with an hourly, daily or monthly basis. Instruments used to measure PM are either Tapered Element Oscillating Microbalance (TEOM 1400ab) or beta monitors; CO is measured with infrared radiation absorption at a wavelength of 4.6 microns. Nitrogen oxide ($NO–NO_2–NO_x$) levels in the atmosphere are measured using chemiluminescent technology, which relies on the fact that nitric oxide (NO) reacts with ozone (O_3), generating IR luminescence with intensity linearly proportional to the NO concentration. Ozone is measured with Thermo Fisher Scientific Model 49*i* Ozone Analyzers, using UV absorption at 254 nm. Sulfur dioxide is measured with Thermo Fisher Scientific Model 43*i* Pulsed Fluorescence SO_2 Analyzers. An additional station located at the campus of the University of Santiago (USACH), near downtown was used to monitor different aerosol components. Non-refractory nitrate, sulfate, ammonium, chlorine and organic matter (OM) in sub-micron particles was measured, from 9 March–4 July 2012, with an Aerosol Chemical Speciation Monitor (ACSM; Aerodyne Research, Billerica, MA, USA). ACSM mass calibration was carried out prior to field measurements, following the procedure indicated in Ng *et al.* (2011). Briefly, calibration determinates the instrument response factor by using ammonium nitrate solution in order to generate monodisperse 300 nm ammonium nitrate aerosol particles. Ammonium nitrate is used as the primary mass calibration. The calibration system utilized in this study was the same described by Carbone *et al.* (2013). An ultrasonic nebulizer (Model NE-U17; Omron) was used to generate the ammonium nitrate particles from solution calibration, which were then passed through a silica gel diffusion dryer (DDU 570/L; Topas), and to a 28 cm long Hauke-type Differential Mobility Analyzer (DMA) and a condensation particle counter (CPC; Model 3010; TSI Inc.). The ammonium nitrate mass concentration was calculated using CPC counts, particle density and diameter, considering spherical particles. The number concentration was varied by diluting the generated aerosol between approximately 10–1000 particles cm^{-3}, which corresponds to the mass concentration of 0.15–15 $\mu g\ m^{-3}$ for nitrate. Elemental carbon (EC) and organic carbon (OC) were resolved with a semi-continuous carbon analyzer (Sunset Laboratory Inc., Portland, OR) from 31 May–4 July 2012, using the NIOSH thermal-optical protocol. This technique involves volatilizing the OC from a quartz filter by ramping up the temperature in steps defined by the NIOSH protocol; subsequently, EC is combusted in an oxygen atmosphere (Chow *et al.*, 1993; Birch and Cary, 1996; Watson *et al.*, 2005; Wu *et al.*, 2016).

The Sunset monitor has a self-calibration routine, but it was also calibrated using a sucrose solution as described in the equipment manual. Aerosol light absorption was measured with a Simca optical monitor from 9 March–4 July 2012. This instrument has been validated in several previous studies (Gramsch *et al.*, 2004; Gramsch *et al.*, 2013; Gramsch *et al.*, 2016). The EC measurements from the Sunset instrument were used to derive a site-specific mass absorption coefficient which was used to convert the light absorption measured by the Simca instrument to EC-equivalent BC or BC_e (Genberg *et al.*, 2013). This was done in order to make the observations comparable to simulated EC concentrations. The correlation between hourly readings of EC from the Sunset instrument and absorption from the Simca instrument was $R^2 = 0.82$ for the time period 31 May–4 July supporting the validity of this approach for this specific site and set of measurements. Fig. 2 shows the scatter plot of the absorption coefficient measured by the Simca and the thermal EC measured by the Sunset. The mass absorption coefficient (MAC) obtained from the plot is 4.89 $m^2\ g^{-1}$.

Emissions

Three different regional emission inventories developed on behalf of Chile's Ministry of the Environment have been used: V Region 2008 (Ambiosis, 2011), VI Region 2006–2010 (DICTUC, 2008) and RM, 2012 (USACH, 2014). The Region V and VI inventories have been updated to the year 2012 in order to obtain consistent input data for the CTM simulations (USACH, 2014).

The emission database includes estimated primary anthropogenic emissions of PM_{10}, $PM_{2.5}$, NO_x, SO_x, NH_3, CO and VOCs. Emissions of biogenic VOCs from vegetation (isoprene, monoterpenes, sesquiterpenes) based on estimates from the MEGAN model (Guenther *et al.*, 2012) were also included. A summary of the emissions in the study area is given in Table 1.
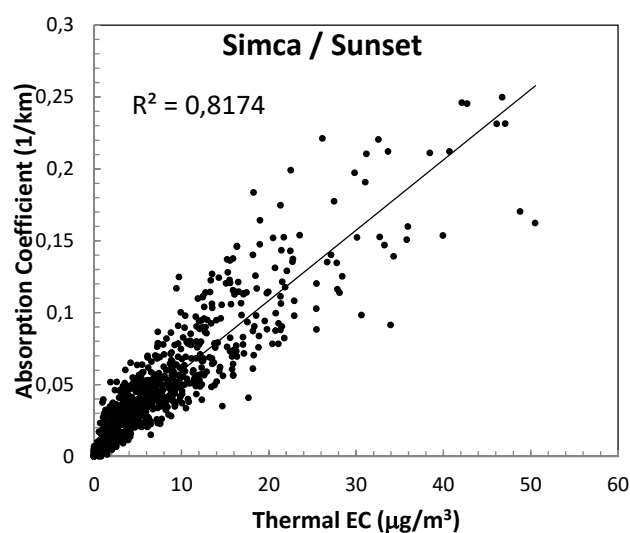

Fig. 2. Scatter plot and correlation between hourly measurements of the optical absorption coefficient by the Simca instrument and thermal EC measured by the Sunset instrument for 31 May–4 July 2012.

The major emitters of PM and CO are fuelwood consumption, industrial sources and forest fires. The major sources of NO_x are associated with the consumption of fossil fuels, mainly from industrial sources and transport, while the largest sources of SO_x are from metal production processes. Major sources of volatile organic compounds (VOCs) include wood combustion, solvent use and storage of fuel (evaporative sources). The dominant sources of NH_3 are related to animal husbandry and the use of fertilizers. Emissions of re-suspended dust from roads could also be important. However, information about these emissions was considered too uncertain and therefore they were not included in the model simulations.

The emission inventory does not include a separation of primary $PM_{2.5}$ into different components of the aerosol. Therefore, a simplified split of the PM emissions into elemental carbon, organic material and other constituents ("dust") was used in the CTM simulations (Table 2). The total VOC emissions were split into individual model VOCs—differences in VOC reactivities influence both the formation of ozone and the formation of secondary organic aerosol. The VOC splits for the different emission sectors were mainly based on Passant *et al.* (2002). Note that both the emission splits are mainly based on estimates for Europe (PM split; mainly Kuenen *et al.*, 2014) and the United Kingdom (VOC split).

The merged and to-year-2012 updated emission database allows estimation of hourly gridded emissions reflecting monthly, daily and diurnal variations for different emission sectors. Apart from gridded emission information the emission database also includes information about more than 1,200 individual point sources (with stack heights and detailed emission data). The 30 largest sources were treated individually in MATCH, modeling the emission height and initial dispersion during the first 10 minutes using an embedded point source model (Langner *et al.*, 1998b). The remaining point sources were averaged horizontally and vertically, into the grid structure used in MATCH, in order to utilize the information on emission height available in the emission database. Hourly emission files for different sectors for both point sources and gridded emissions were used as input to the MATCH simulations. As an example Fig. 3(a) shows the monthly variation of $PM_{2.5}$ emissions aggregated for the Santiago metropolitan region while Fig. 3(b) shows the composite diurnal variation of all the direct $PM_{2.5}$ emissions in the same region. As can be seen emissions are estimated to be higher in winter, mainly due to increasing wood combustion. Average daytime emissions are estimated to be more than twice as high as during nighttime.

Table 1. Emissions for 2012 used in the model simulations, based on regional inventories for Region V (Ambiosis, 2011), Region VI (DICTUC, 2008) and the metropolitan region (USACH, 2014). The V and VI regional inventories have been updated to year 2012 by USACH (2014). Unit: tons year^{-1}.

Emission sector	$PM_{2.5}$	VOC	NH_3	SO_2	CO	NO_x
Stationary combustion and industrial processes	8,300	2,370	1,530	83,420	7,220	24,700
Residential wood combustion	10,400	58,250	830	140	98,500	1,020
Field burning	1,450	1,150	10	60	9,970	430
Wildfires	3,440	3,650	310	280	39,530	1,370
Machinery used in construction	1,100	1,470	0	5,590	7,890	15,450
Fugitive emissions[*]	0	100,620	0	0	190	0
Road traffic light vehicles	900	12,460	2,430	270	144,830	28,420
Road traffic heavy vehicles	1,630	2,190	10	290	10,310	44,380
Agriculture	30	3,300	171,350	0	0	0
Residential heating (excl. wood)	10	30	220	320	470	1,810
Biogenic	0	46,870	0	0	0	0
Sum	28,060	232,360	176,690	90,360	318,900	117,580

[*] From petrol stations, fuel storage, dry cleaners, car painting, coatings.

Table 2. Splits of primary PM emissions into elemental carbon (EC), organic matter (OM) and other (non-carbonaceous) components ("dust") for different emission sectors, used in the model simulations. The splits are based on Reid *et al.* (2005), Akagi *et al.* (2011) and Kuenen *et al.* (2014).

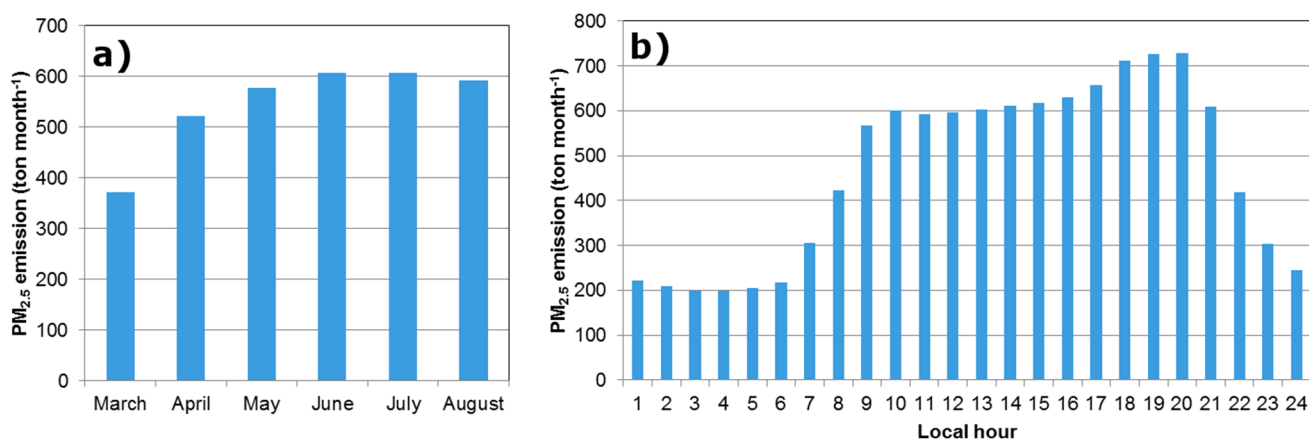| Emission sector	EC %	OM %	Dust %
Stationary combustion and industrial processes	7	7	86
Residential wood combustion	9	62	29
Field burning	6	87	7
Forest fires	4	87	9
Machinery	43	32	25
Road traffic light vehicles	29	53	17
Road traffic heavy vehicles	67	25	8
Agriculture	0	32	68
Residential heating (excl. wood)	10	90	0

Fig. 3. (a) Monthly variation of $PM_{2.5}$ emissions for the Santiago metropolitan region (area of the region indicated in Fig. 1) and (b) composite diurnal variation of the $PM_{2.5}$ emissions in the same region.

Chemical Transport Model

For this study we used the MATCH CTM, which previously has been used to study sulfur air pollution in central Chile, as well as arsenic dispersion from mining activities across Chile (Gallardo *et al.*, 2002; Gidhagen *et al.*, 2002; Olivares *et al.*, 2002). The present version of the MATCH CTM also includes schemes for photochemical oxidants and particulate matter. The basic structure of the MATCH model, along with the methodology of balancing the three-dimensional wind field and calculating turbulent mixing and advection with the mean wind, is described by Robertson *et al.* (1999).

The gas-phase chemistry is based on the EMEP MSC-W EmChem09 scheme of Simpson *et al.* (2012), with reaction rates updated following the recommendations by the International Union of Pure and Applied Chemistry (IUPAC) (Atkinson *et al.*, 2006; Andersson *et al.*, 2015), and with a modified mechanism for isoprene chemistry based on an adapted version of the Carter one-product mechanism (Carter, 1996; Langner *et al.*, 1998a). A dozen representative compounds are used to represent all hydrocarbons emitted to the atmosphere. The photolysis rates depend on the photolytically active radiation, which is calculated from latitude, height, time of day and cloud cover (Moldanová *et al.*, 2002).

The aerosol scheme in the model includes gas-to-aerosol conversions creating secondary inorganic aerosol (SIA; ammonium sulfate and nitrate) and secondary organic aerosol (SOA). The latter are divided into biogenic SOA (BSOA; from isoprene, monoterpenes and sesquiterpenes) and anthropogenic SOA (ASOA; mainly from aromatic hydrocarbons). Primary organic aerosol emissions are treated as non-volatile in the model. The SOA scheme is a modified version of one of the volatility basis set (VBS) schemes used by Bergström *et al.* (2012). The scheme with "No Gas-particle partitioning of primary organic aerosol (POA) emissions" (i.e., treating POA as non-volatile) and "No Aging reactions of SOA" (VBS-NPNA scheme) was used in the present study, but with a background organic aerosol, OA, concentration of 0.4 µg m^{-3}, and including SOA from sesquiterpenes with a 17 wt% SOA yield (based on Mentel

et al., 2013). Aerosol concentrations are modeled using two size bins, fine and coarse, separating aerosol particles smaller and larger than 2.5 µm in diameter. Simulation of sea salt aerosols was not included in the model setup since the focus was on the situation inland and on $PM_{2.5}$. Observed concentrations of sodium, Na, a sea salt tracer, are reported to be low in the $PM_{2.5}$ fraction in Santiago, 104 ng Na m^{-3} as a winter average (April–September, 1998–2007) at the station Parque O'Higgins (Moreno *et al.*, 2010). Assuming that all sodium in these observations comes from sea salt and a using a fraction by weight of sodium in sea salt of 30.61% (Seinfeld and Pandis, 2016), implies an average sea salt concentration of 340 ng m^{-3} or on the order of 1% of the observed total winter average $PM_{2.5}$ at the station. The corresponding concentration of sea salt in PM_{10} was more than three times larger or 1.3 µg m^{-3}. Concentrations of Na are higher closer to the Pacific coastline. Gidhagen *et al.* (2002) report 1,652 ng Na m^{-3} in the PM_{10} fraction as a 1-year average in Quillota ~25 km from the Pacific coast (Fig. 1) corresponding to a concentration of sea salt of 5.4 µg m^{-3} or about 10% of the observed PM_{10}. Using the same relation between Na in $PM_{2.5}$ and PM_{10} as observed by Moreno *et al.* (2010) implies a sea salt concentration in $PM_{2.5}$ of 1.4 µg m^{-3} in Quillota.

Low (seasonally constant) concentrations of all pollutants were used on the boundaries, assuming very clean conditions in the Southern Hemisphere, based on global CTM re-analysis from the Copernicus Atmospheric Monitoring Service (Flemming *et al.*, 2017) and published observations (e.g., Seinfeld and Pandis, 2016).

Meteorological Fields

Three-dimensional meteorological data needed for the CTM simulations were taken from operational forecast runs of the WRF-Chem model (Grell *et al.*, 2005; Skamarock *et al.*, 2008) performed by the National Weather Service in Chile (Delgado *et al.*, 2014). Version 3.1.1 of WRF-Chem was used on three nested grids using 2, 6 and 18 km horizontal resolution respectively. The model has 39 vertical levels up to 100 hPa, with a first layer of 10 m thickness, and six levels below 100 m. Model forecasts out to 5 days were

run daily using initial and boundary conditions for the first 24 hours from the National Centers for Environmental Prediction (NCEP) Final Global Operational Analysis at 1° horizontal resolution (FNL, http://rda.ucar.edu/datasets/ds0 83.2/) and boundary conditions from Hour 25 to 120 from NCEP Global Forecasting System (GFS) at 0.5° horizontal resolution (GFS, http://rda.ucar.edu/datasets/ds084.6/). Only the first 24 hours were used in the CTM simulations. Due to storage constraints the full three-dimensional data needed for the CTM could only be saved for a limited time period. The available meteorological data covers the period from 9 March–21 August 2012 (i.e., 166 days).

RESULTS

Observed and Simulated Meteorological Conditions

A good simulation of the meteorological conditions is necessary for the CTM modeling. Here we focus on evaluating surface wind direction and speed from the meteorological model since this has a major impact on simulated surface concentrations of $PM_{2.5}$ in the region. The geographical setting, with highly complex terrain surrounding the Santiago Basin, strongly influences meteorology and the dispersion of primary and secondary contaminants in the region.

In the absence of strong synoptic disturbances, the wind patterns in the region are characterized by diurnally varying mountain-valley wind systems. The nighttime downslope winds are strongest at higher levels on the slopes of the Andes. They get weaker as they reach the lower part of the basin and winds are generally light during nighttime inside the basin. During daytime the wind patterns are organized due to pronounced upslope and up-valley winds; usually westerly to southwesterly winds prevail in the basin.

Fig. 4 illustrates the observed and simulated variation of the surface wind direction at the station Talagante located to the southwest of Santiago in the Maipo River valley and Fig. 5 shows the corresponding information for the station Parque O'Higgins inside Santiago. Data for two 2-week periods in 2012 are plotted. The first period in March corresponds to late summer/fall conditions and the second period in July corresponds to winter conditions. The diurnal pattern is most pronounced during the winter and it is more distinct at Talagante. In the summer/fall period the daytime westerly winds prevail during a larger fraction of the day while in the winter the nighttime easterly wind becomes a more dominating feature. The meteorological model simulates the variation in wind direction quite well. The performance is better at Talagante than at Parque O'Higgins and also better in the winter period when diurnal variations are more pronounced.

Fig. 6 shows the observed and simulated diurnal variation of the wind speed for the same stations and time periods. Average wind speeds are low with observed average daily maximum values around 2.5 m s⁻¹ in the summer/fall period and less than 1.5 m s⁻¹ in the winter period. A good simulation of such low wind speeds is a challenge for the meteorological model. The simulated diurnal cycle of the wind speed at Talagante is similar to the observed, but with an overestimation of peak wind speeds during afternoon by about 1 m s⁻¹ in the summer/fall period. At Parque O'Higgins daytime wind speeds are close to the observed, but nighttime wind speed is overestimated by about 0.5–1 m s⁻¹ in the winter period.

In Table 3 we compare observed and simulated mean wind speeds for the two time periods for Talagante and Parque O'Higgins as well as for two additional surface stations in Santiago (Quinta Normal and Independencia) and
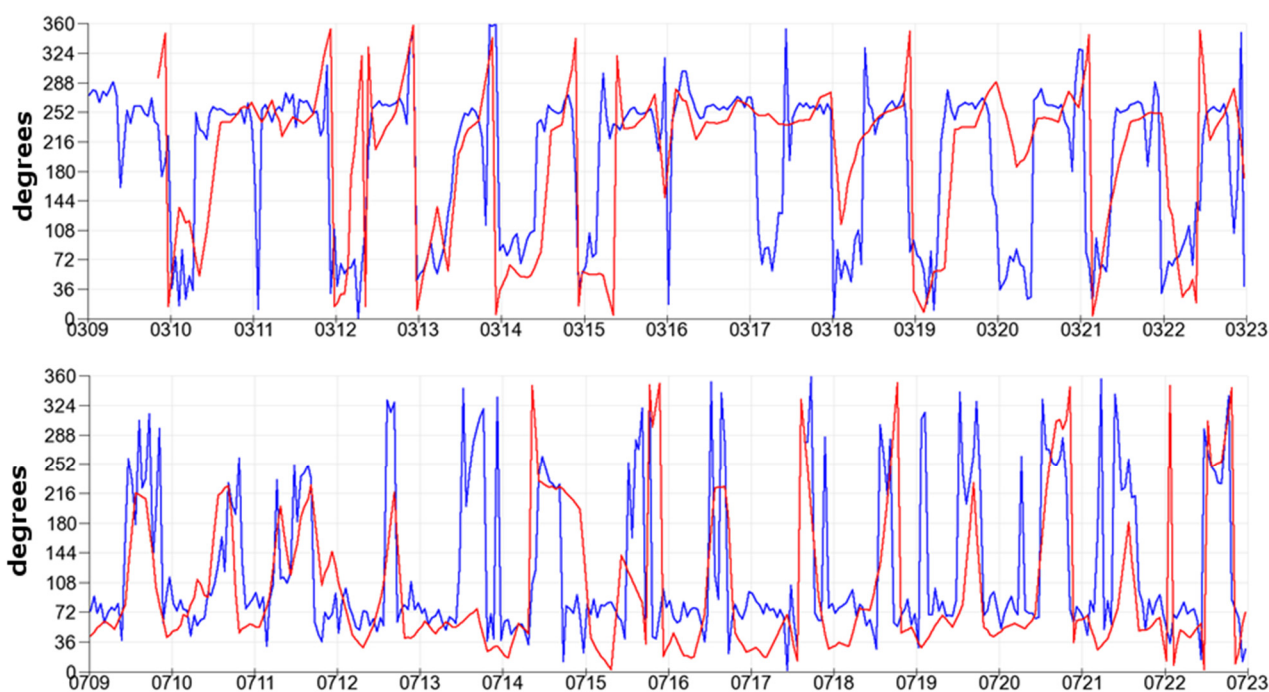

Fig. 4. Comparison between the wind direction measured (blue) and simulated by the WRF-Chem model (red) at Talagante for 2 weeks during the summer/fall (top) and during the winter (bottom).
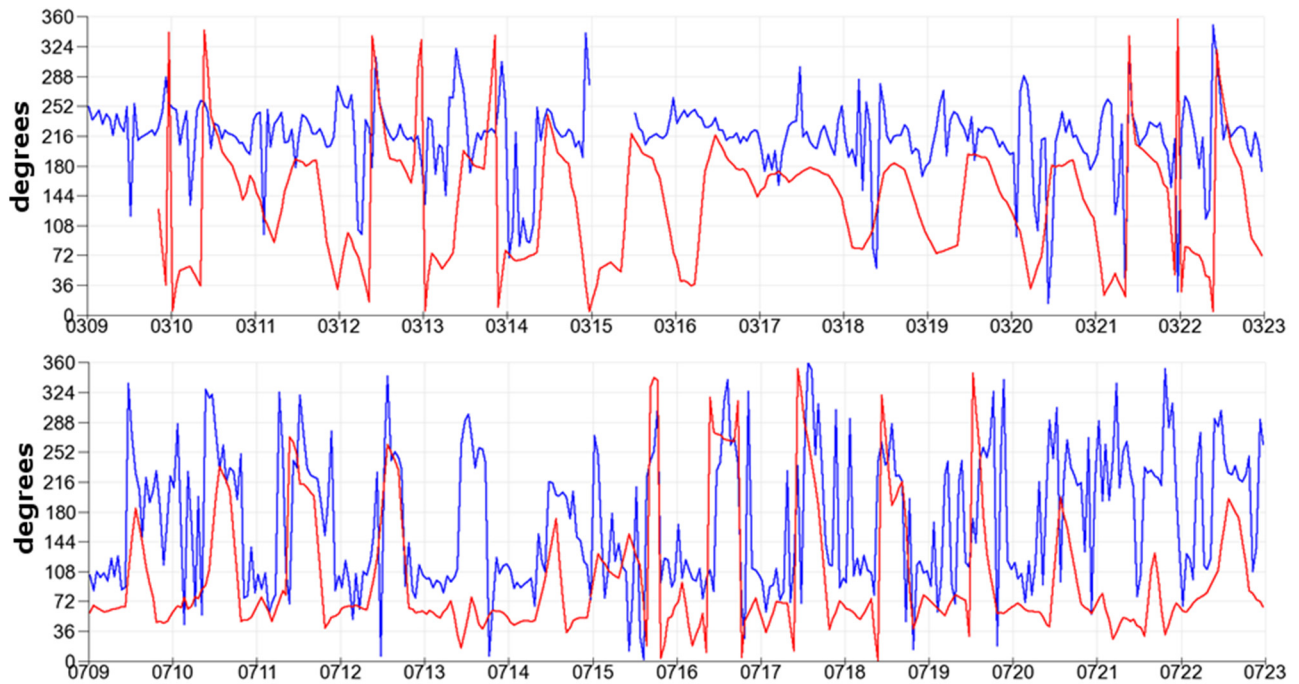
Fig. 5. Comparison between the wind direction measured (blue) and simulated by the WRF-Chem model (red) at Parque O'Higgins for 2 weeks during the summer/fall (top) and during the winter (bottom).
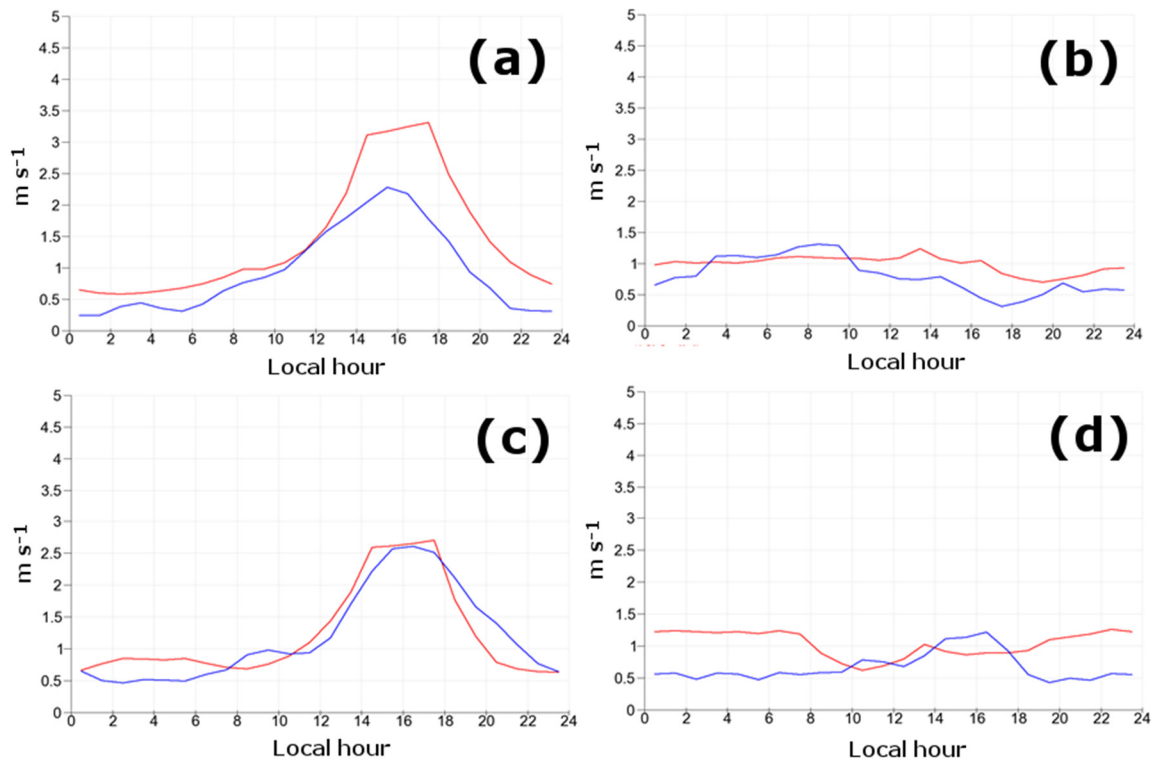

Fig. 6. Comparison between the diurnal variation of the wind speed measured (blue) and simulated by the WRF-Chem model (red) at Talagante for (a) 9–22 March 2012 and (b) 9–22 July 2012 and at Parque O'Higgins for (c) 9–22 March 2012 and (d) 9–22 July 2012.

three stations in Region V (Los Vientos, Loncura and Viña del Mar), see Fig. 1. Simulated mean wind speeds are equal or slightly higher than observed at the stations located close to (Talagante) and inside (Independencia and Parque O'Higgins) Santiago but considerably lower at one station, Quinta Normal. At the inland station Los Vientos (in the

north) the simulated mean wind speed is almost equal to the observed wind speed in winter but underestimated in summer. Along the coast, to the northwest, simulated mean values are higher than observed especially at Viña del Mar, which has the lowest observed mean wind speed of all stations studied here.

Precipitation is generally important for the simulation of $PM_{2.5}$ and precursors. Precipitation amounts in central Chile are however quite low. Observed 30-year average annual precipitation in Santiago is below 300 mm and in 2012 the annual precipitation in Santiago was below 200 mm (DMC, 2019). Fig. 7 shows a comparison between observed and simulated daily precipitation at the station Pudahuel in western Santiago for the period 26 April–20 August 2012. There were only small amounts, < 1 mm, observed and simulated on 3 of the days before the 26th April. The WRF-Chem simulation captures the main observed rainy episodes and simulates precipitation for 22 of the 28 days when precipitation was observed at Pudahuel during the study period of 166 days. Precipitation is however simulated for an additional 11 days when there was no precipitation observed so the number of rainy days in Santiago are overestimated in WRF-Chem even though the frequency of precipitation days is below 20%. The additional rainy days in the simulation occurs in connection with the observed rainy periods apart from one episode in the beginning of August when no precipitation was observed.

Observed and Simulated Pollutant Concentrations

Observed and simulated mean concentrations of NO_x,
SO$_2$, O_3 and $PM_{2.5}$ are given in Table 4. The stations are ordered from north to south with most of the stations located inside the Santiago urban area. Simulated concentrations are within 50% of the observed values for the majority of the stations inside Santiago for NO_x, SO_2, O_3 and $PM_{2.5}$. Simulated concentrations of $PM_{2.5}$ are however lower than observed at all stations in Santiago and at three of the eight stations the difference is larger than 50%. The underestimation is probably due to a combination of factors. Simulated wind speeds are too high leading to too rapid ventilation of primary emissions. The lack of emissions from re-suspended road dust in the simulation probably also explain part of the difference. As will be discussed further below, the concentration of organic matter in the simulations are lower than observed by about 4.5 µg m^{-3} at the USACH station inside Santiago; this could be due to underestimated direct emissions of organic aerosol particles or missing emissions of semi- and intermediately volatile organic compounds (SVOCs and IVOCs) that could lead to secondary aerosol formation (e.g., Robinson *et al.*, 2007; Ots *et al.*, 2016). Underestimated emissions of OM in the model simulations could potentially explain a fairly large part of the underestimated $PM_{2.5}$ concentrations at least at some locations. For the stations in Region V the results are mixed, with deviations larger than 50% for most comparisons. This could partly be due to model resolution in relation to these smaller urban settings. It should be kept in mind that the grid resolution of the CTM is 2 × 2 km^2 and that all stations are located inside, or close to, areas with human activity, so model resolution can clearly be an issue in the vicinity of strong emission gradients. Very large deviations

Table 3. Comparison between averaged wind speed as observed and as simulated by the WRF-Chem model during a 2-week summer and winter period. Unit: m s^{-1}.

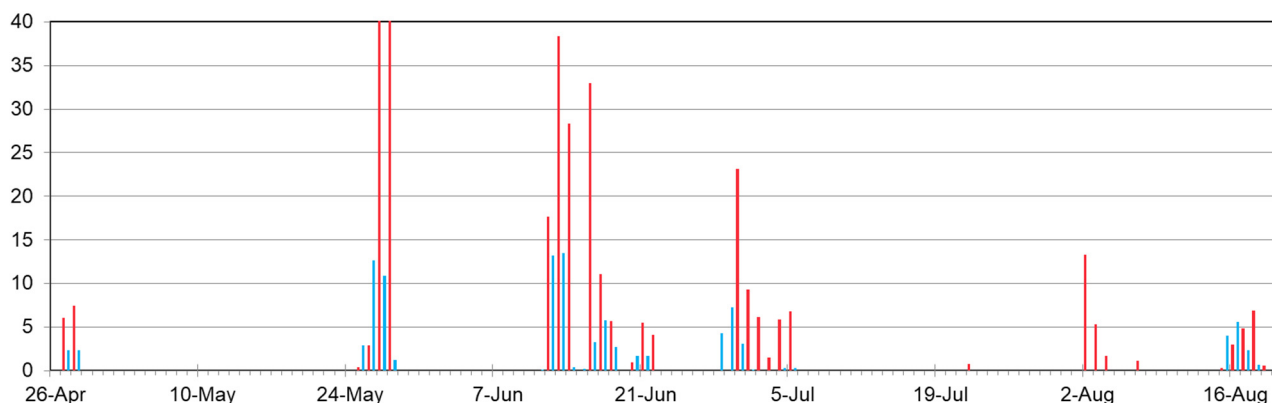|	Independencia	Quinta Normal	Parque O'Higgins	Talagante	Los Vientos	Loncura	Viña del Mar
Summer/Fall (9–22 March 2012)							
Obs.	1.1	3.4	1.2	0.9	3.7	1.3	0.5
Sim.	1.3	1.3	1.2	1.5	2.5	2.0	2.8
Winter (9–22 July 2012)							
Obs.	0.7	1.8	0.7	0.8	1.8	1.2	0.4
Sim.	1.0	1.0	1.0	1.0	1.7	1.7	3.5

Fig. 7. Comparison between the daily precipitation measured (blue) and simulated by the WRF-Chem model (red) at the station Pudahuel for the period 26 April–20 August 2012. High daily precipitation amounts of 51 and 72 mm were simulated on the 27th and 28th May respectively. Observation data from DMC (2019).

Table 4. Observed and simulated mean concentrations of NO_x, SO_2, O_3 and $PM_{2.5}$ in the study region for the period 9 March–21 August 2012. Evaluation based on hours for which both measurements and simulated data were available. Note that for Region V monitored $PM_{2.5}$ data were only available for 3 weeks in July–August 2012 (values in parentheses). For the SO_2 measurements a constant offset of 2.62 µg m^{-3} has been deducted from all hourly values and for zero hourly values a value corresponding to half of the detection limit, 1.31 µg m^{-3}, has been assumed (SINCA, 2018). Blue, orange and red shading indicate deviations between observed and simulated vales by < 25, < 50 and > 50% respectively. Unit: µg m^{-3}.

Station	NO$_x$		SO$_2$		O$_3$		PM$_{2.5}$	
	Obs.	Sim.	Obs.	Sim.	Obs.	Sim.	Obs.	Sim.
Region V, NW part								
La Greda	41.3	126.5	11.4	282.6	14.6	21.0	(16.3)	(63.7)
Los Maitenes	28.9	57.5	26.0	117.0	16.7	29.1	(11.1)	(29.9)
Viña del Mar	–	63.3	–	6.1	7.5	28.1	(18.4)	(13.9)
Metropolitan region, Santiago urban area								
Quilicura	177.5	153.0	1.6	1.8	19.5	14.2	33.0	18.4
Las Condes	117.5	61.7	–	0.9	21.1	24.0	23.4	9.6
Independencia	233.5	204.8	1.8	1.3	14.3	9.3	30.0	17.9
Parque O'Higgins	207.4	277.2	6.8	1.3	19.4	8.1	34.7	21.5
El Bosque	226.9	205.0	1.2	1.7	18.6	13.1	38.0	16.9
La Florida	168.3	126.8	0.6	1.4	18.2	14.2	32.7	13.2
Pudahuel	215.1	201.2	–	2.2	17.2	11.8	39.1	25.1
Puente Alto	122.9	86.5	1.3	1.9	21.3	21.3	30.6	16.2
Metropolitan region SW part and Region VI								
Talagante	76.4	32.9	1.9	2.3	21.8	39.3	29.2	18.5
Rancagua	–	19.8	–	4.8	–	37.1	52.1	42.2

are evident for the stations La Greda and Los Maitenes. These two stations are located close to the large point sources of the Ventanas industrial complex, and the model has difficulties in correctly simulating the vertical gradients of concentrations in the plumes from the high stacks in the area. Moreover, according to the emission inventory, a large fraction of these industrial emissions occur close to the surface—this may be an unrealistic assumption. Observed and simulated mean concentrations of ozone in Santiago are mostly below, or close to 20 µg m^{-3}, which is typical for the period of the year. At the stations outside Santiago (e.g., at Talagante) the model simulates higher ozone concentrations than observed in most cases, indicating either some photochemical production or problems related to model resolution. Too high boundary concentrations on the western border could also be a reason.

Next we turn to a more detailed discussion of the concentrations of $PM_{2.5}$ in Santiago. Observation studies have shown that Parque O'Higgins is the most representative station of the air quality network in Santiago (Gramsch *et al.*, 2006; Henriquez *et al.*, 2015) and Fig. 8 shows observed and simulated diurnal average values of $PM_{2.5}$ at this station for the whole simulated period. During summer/fall observed and simulated levels are very similar, but during the winter the model does not always manage to simulate the peak levels. Periods with higher dilution (lower levels) in winter are however well simulated indicating the ability of the meteorological model to capture the synoptic variability in a good way. Fig. 9 shows the observed and simulated mean diurnal variation of $PM_{2.5}$ at the same station for 2 weeks in summer/fall and in winter. It is clear that the CTM does not manage to simulate high enough levels during nighttime in the winter period. Also emissions seem to be too high in the evening since the model simulation has a peak in the

concentrations at this time of day both in summer/fall and in winter. These discrepancies can partly be related to over-prediction of wind speeds in WRF-Chem at nighttime during winter as discussed above. The description of the diurnal variations in the emission database is another factor that is of importance, especially for the simulated peak in the evening, which to a large extent is driven by residential wood burning emissions.

Fig. 10 shows time series of observed diurnal average concentrations of different aerosol components measured at the USACH station. This station is located about 2 km to the northwest of the station Parque O'Higgins. Observations overlapping the CTM simulations cover the period 9 March–4 July. As for other stations in Santiago the observed concentrations are higher in the winter period and lower in summer/fall. Focusing on the winter part of the period, 31 May–4 July, organic matter is the dominating component, contributing 51% to the total measured particle mass by the ACSM and Simca instruments, followed by BC$_e$ at 21%, nitrate at 17%, ammonium at 8%, sulfate at 2% and chlorine at 2%. These fractions are rather similar to those reported by Tagle *et al.* (2018) in the winter of 2016 at Pudahuel, close to the airport in the western part of Santiago, and at Las Condes in the eastern part. Fractions of OM were 67 and 48%, followed by nitrate at 13 and 30%, BC$_e$ at 9 and 8%, ammonium at 6 and 11%, sulfate at 2% and chlorine at 2 and 1% respectively for these two stations. Villalobos *et al.* (2015) report chemical speciation of $PM_{2.5}$ for 2013 based on chemical analysis of filter samples and source apportionment of OC for a rooftop station in central Santiago about 8 km southeast of the USACH station. The observed averages in June 2013 were 59% for OM, 19% for nitrate, 11% for EC, 7% for ammonia, 3% for sulfate and 2% for other components.
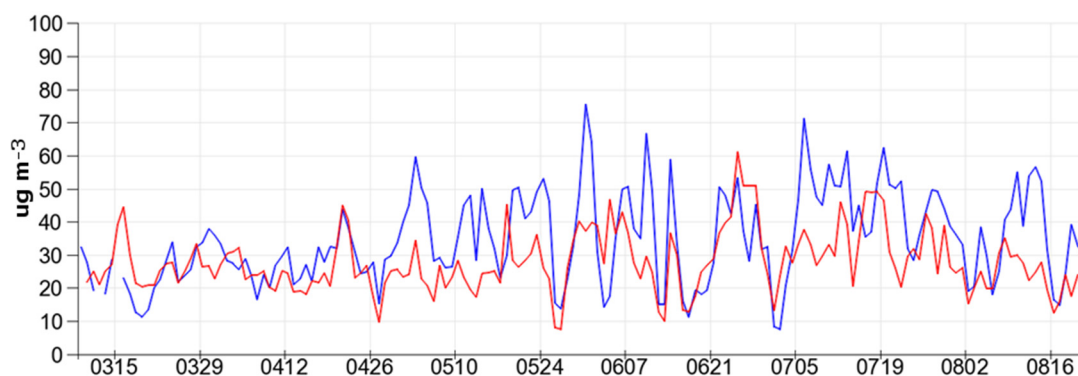
Fig. 8. Observed (blue) and simulated (red) diurnal average concentrations of PM$_{2.5}$ at the station Parque O'Higgins for the period 9 March–21 August 2012. Unit: µg m^{-3}.
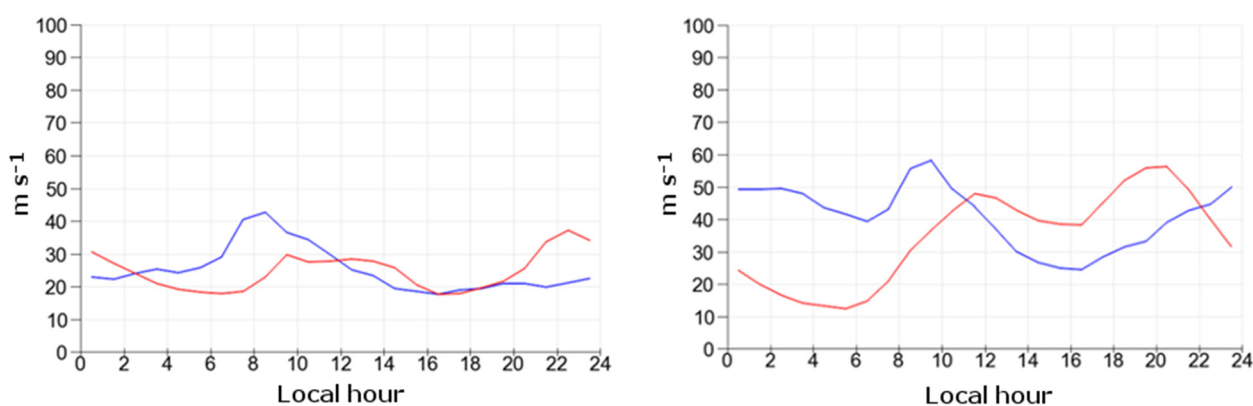

Fig. 9. Observed (blue) and simulated (red) diurnal variation of concentrations of PM$_{2.5}$ at the station Parque O'Higgins for the period 9 March–8 April (left) and 9 July–8 August (right). Unit: µg m^{-3}.
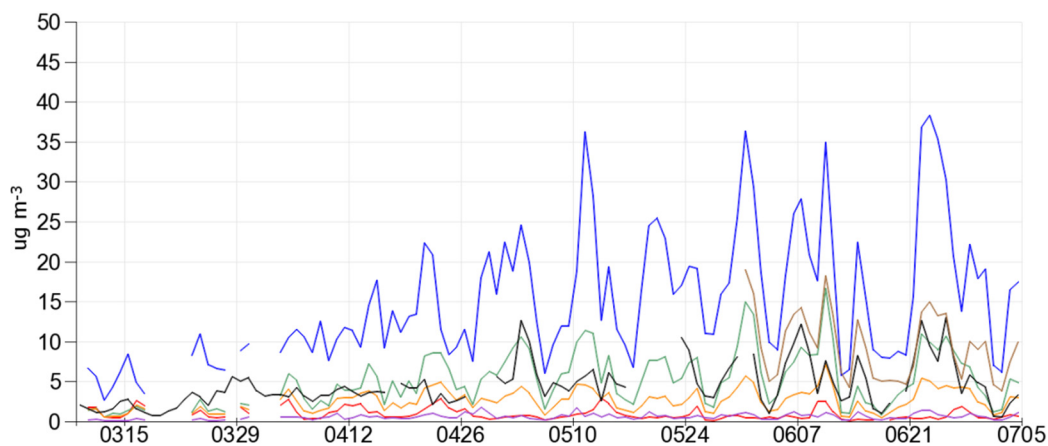

Fig. 10. Observed diurnal average concentration of organic matter (blue), organic carbon (brown), nitrate (green), ammonium (yellow), sulfate (red), chlorine (pink) and BC$_e$ (black) at the USACH station for the period 9 March–4 July. Unit: µg m^{-3}.

For March–August 2013 corresponding numbers were 59, 18, 10, 8, 5 and 2% respectively (data extracted from Fig. 2 and from the supplement in Villalobos *et al.*, 2015). The fraction of BC$_e$ presented here for USACH is a factor of two higher than observed for BC in Tagle *et al.* (2018) and for EC in Villalobos *et al.* (2015). The difference in observed concentrations is however less. Tagle *et al.* (2018) report 4.35

and 3.23 µg m^{-3} for Pudahuel and Las Condes respectively while Villalobos *et al.* (2015) report 8.7 µg m^{-3} in June 2013 and 5.0 µg m^{-3} as an average for March–August 2013. Observed BC$_e$ at USACH was 6.2 and 7.7 µg m^{-3} for the periods 9 March–21 August and 31 May–4 June 2012 respectively (Table 5).

Model-simulated average chemical composition of PM$_{2.5}$

at USACH for different periods are given in Table 5. Here we compare simulated EC with observed BC_e from the Simca instrument as well as with thermally determined EC from the Sunset instrument. Qualitatively the relations between OM, SIA components and BC_e are well simulated, with the organic fraction being the largest, followed by EC. A pie chart illustrating observed and simulated contributions for the period 9 March–4 July is shown in Fig. 11. For this period the largest differences in concentrations are seen for the organic fraction which is underestimated by 4.7 µg m^{-3} (32%), while BC_e is overestimated by 1.5 µg m^{-3} (24%). This indicates that the assumed split of primary PM emissions into organic matter, elemental carbon and dust for different sectors in the emission inventory may be unrealistic for some sources. The simulated concentration of PM$_{2.5}$ at USACH is dominated (90%) by emissions from light- and heavy-duty vehicles. Shifting the split of the vehicle emissions towards less EC and more OM could be one way of improving the simulated concentrations at USACH. However, as discussed above, an alternative explanation for too little organic matter in the simulation is underestimated SOA, e.g., due to missing SVOC or IVOC emissions. Most of the simulated organic matter originates from primary emissions, with a contribution from secondary organic aerosol from oxidation of VOC emissions of less than 10% inside Santiago. This is likely an underestimation of the SOA fraction. For the period with simultaneous measurements of OM and organic

carbon the model-simulated ratio OM:OC is about 1.51 while the measurements indicate a much higher ratio: 1.96. OM:OC ratios of around 2 corresponds to a relatively high degree of oxidation, and could be an indication of a relatively aged organic aerosol with a large fraction of SOA. Organic matter emitted from biomass combustion may also have high OM:OC ratios (e.g., Turpin and Lim, 2001; Aiken *et al.*, 2008) so another possible reason for the underestimated OM:OC ratio could be underestimated emissions from wood combustion or burning vegetation. OM:OC ratios for primary OA emissions from diesel and gasoline vehicles are expected to be low (~1.25; Aiken *et al.*, 2008) and thus a shift of the emission split for road traffic from EC to OM would lead to even worse agreement between the modeled OM:OC ratios and the measurements at USACH. The modeled particulate total carbon (TC) concentration (18.6 µg C m^{-3}) is in good agreement with the measured TC (17.3 µg C m^{-3}) at the USACH station (for 31 May–4 July).

The simulated concentrations of inorganic aerosol components at USACH are lower than observed for all components; sulfate by 0.1 µg m^{-3} (11%), nitrate by 1.6 µg m^{-3} (31%) and ammonium by 1.3 µg m^{-3} (50%), considering the whole period of observation. Considering only the winter part of the observation period, 31 May–4 July, the differences between the measured and simulated inorganic aerosol components are larger, with 29, 71 and 77% lower simulated concentrations for sulfate, nitrate and

Table 5. Observed and simulated average concentrations and contributions to PM$_{2.5}$ from different aerosol components at the USACH station for different time periods in 2012. Columns OC_{ss} and EC_{ss} are observed data from the Sunset instrument. TC_{ss} is the sum of OC_{ss} and EC_{ss}. BC_e is data from the Simca instrument and observed OM, SO$_4$, NO$_3$, NH$_4$ and Cl are from the ACSM instrument. The observed sum is given as the sum of OM, SO$_4$, NO$_3$, NH$_4$, Cl and BC_e as measured by the ACSM and Simca instruments. The simulated sum is given by the sum of OM, SO$_4$, NO$_3$, NH$_4$ and EC. Unit: µg m^{-3}.

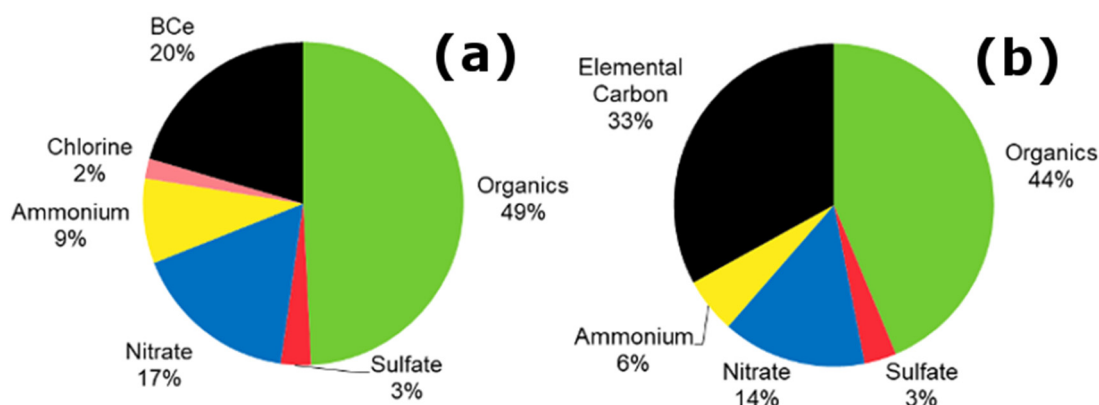| Period		OM	OC$_{ss}$	SO$_4$	NO$_3$	NH$_4$	Cl	BC$_e$/EC	EC$_{ss}$	TC$_{ss}$	Sum
9 Mar–4 Jul	Obs.	14.9	–	0.9	5.1	2.6	0.6	6.2	–	–	30.3
	Sim.	10.2	6.6	0.8	3.4	1.3	–	7.7	7.7	14.3	23.4
31 May–4 Jul	Obs.	18.8	9.6	0.7	6.2	3.0	0.7	7.7	7.7	17.3	37.1
	Sim.	13.3	8.8	0.5	1.8	0.7	–	9.8	9.8	18.6	26.1
9 Mar–21 Aug	Sim.	10.5	6.9	0.8	3.2	1.2	–	8.0	8.0	14.9	23.7
9 Mar–9 Apr	Sim.	6.9	4.6	1.5	6.7	2.5	–	6.3	6.3	10.9	23.9
22 May–21 Aug	Sim.	12.2	8.1	0.5	2.0	0.8	–	9.0	9.0	17.1	24.5

Fig. 11. (a) Observed and (b) simulated contributions to PM$_{2.5}$ (excluding dust) at the USACH station for the period 9 March– 4 July. The sums of observed and simulated components are 28.6 and 23.4 µg m^{-3} respectively.

ammonium respectively. A possible explanation for this is that oxidation of NO_x to HNO_3 is too slow in the model. A sensitivity study with increased ammonia emissions did not result in substantially higher concentrations of ammonium, so underestimated ammonia emissions do not seem to be the main problem.

Simulated statistics at USACH (Table 5) are also given for the whole simulated period, 9 March–21 August, as well as for the summer part, 9 March–9 April, and the winter part, 22 May–21 August. For the whole period the simulated fractions of different aerosol components are similar to those simulated for the shorter period with observations. For summer conditions the CTM simulates higher concentrations and fractions of inorganic components, compared to the winter period, and lower concentrations and fractions of organic matter, elemental carbon and dust. Increased concentrations of inorganic components are expected in summer due to faster oxidation of the primary emitted gaseous components and larger emissions of ammonia.

Fig. 12 shows maps of simulated total $PM_{2.5}$ for the period 9 March–21 August 2012, as well as contributions from primary emissions from different sectors, and contributions from all sectors to SIA (sulfate, nitrate, ammonium) and SOA. Primary contributions from traffic and machinery dominate in the Santiago urban area and along the main traffic routes to the north, south and west—the maximum contributions are in excess of 10 µg m^{-3}. Contributions from traffic and machinery are also visible in the Valparaiso/Viña del Mar region but the maximum contributions are much smaller here than simulated in Santiago, on the order of 1–2 µg m^{-3}. Residential wood combustion is dominating in other urban areas than Santiago, and also in the outskirts of Santiago, with contributions in excess of 10 µg m^{-3} in many places. Residential wood combustion also contributes with a substantial background concentration of $PM_{2.5}$ of 1–2 µg m^{-3} over a large fraction of the model domain. Primary industrial emissions give high contributions, exceeding 10 µg m^{-3} in the vicinity of the major sources, in particular to the north in Region V, in connection with the Ventanas industrial complex on the coast, and at several locations of point sources further inland in the north. In the mountains northeast of Santiago there is also a strong contribution from primary industrial emission exceeding 10 µg m^{-3}, due to open mining activities in the area. Primary emissions from wildfires and/or agricultural burning are of some importance in the southwestern part of the domain but simulated contributions are generally below 2 µg m^{-3}. Secondary inorganic aerosol is the dominating aerosol component, in areas without primary emissions, with contribution in excess of 5 µg m^{-3} over a large part of the model domain. Maximum contributions in excess of 10 µg m^{-3} are simulated in connection with the large point sources in the north and in the southeastern part of the domain. Simulated contributions from biogenic secondary organic aerosol are small, below 0.2 µg m^{-3}, while simulated contributions from anthropogenic secondary organic aerosol are larger, reaching above 0.5 µg m^{-3} in some urban locations. In general, the model-simulated contribution from SOA is much smaller than the contributions from primary emissions and secondary inorganic aerosol.

CONCLUSIONS

Using a regional CTM, we have simulated the concentrations and chemical composition of $PM_{2.5}$ as well as its contributions from various emission sectors in the central region of Chile from March to August of 2012, a period that encompasses late summer, fall and winter conditions, when $PM_{2.5}$ concentrations peak. Meteorological data for the CTM were obtained from operational model runs at the National Weather Service in Chile using the WRF-Chem model. The simulated surface wind fields show good agreement with the observations in terms of seasonal, synoptic and daily variations in the wind speed and direction, but the speeds estimated by WRF-Chem exceed those observed during nighttime in the metropolitan region. The timing of precipitation episodes in Santiago, except for one period at the beginning of August, is accurately predicted.

The simulated mean concentrations of the gaseous precursors NO_x and SO_2, as well as ozone, fall within 50% of the observed values for the majority of stations in the metropolitan region of Santiago, indicating that the total anthropogenic emissions of precursor gases are realistically described in the emission inventory for this region. However, the $PM_{2.5}$ concentrations are underestimated by more than 50% for three of the eight stations in Santiago, which may be caused by an underestimation of direct $PM_{2.5}$ emissions—or SOA precursor emissions—but can also be attributed to overly high wind speeds in the CTM simulations. The discrepancies between the simulated and the observed mean concentrations are larger in Regions V and VI, the neighboring regions to the north and south of Santiago, respectively; the poorer agreement in these regions may be due to the relatively coarse geographical resolution of the CTM.

The simulated winter $PM_{2.5}$ concentrations in Santiago are lower and higher than the values observed during nighttime, and daytime and late evening, respectively; these differences may be related to excessive simulated wind speeds, as well as to uncertainties in the diurnal variation in the emissions. During summer, the simulated diurnal variation better agrees with the observations, but the peak concentrations during the morning are underestimated, whereas those during the evening are overestimated.

The simulated concentrations of chemical components in the $PM_{2.5}$ at the USACH station in Santiago for 9 March–4 July are all lower than the observed values, except for EC and BC_e, which are overestimated by the model. The largest discrepancies exist for OM and BC_e, the predictions of which differ from the observed concentrations by 4.7 µg m^{-3} (–32%) and 1.5 µg m^{-3} (+24%), respectively. The primary $PM_{2.5}$ emissions are split into individual aerosol components for the CTM simulation; this split may be a source of error in the estimation of OM. Additionally, missing emissions of SVOCs and IVOCs, which result in the formation of SOA, are another potential factor. The simulated mean concentrations of sulfate, nitrate and ammonium—inorganic aerosol components—for the entire observation period, 9 March–4 July, fall short of the observed values by 0.1 µg m^{-3} (–11%), 1.6 µg m^{-3} (–31%) and 1.3 µg m^{-3} (–50%), respectively; furthermore, poorer
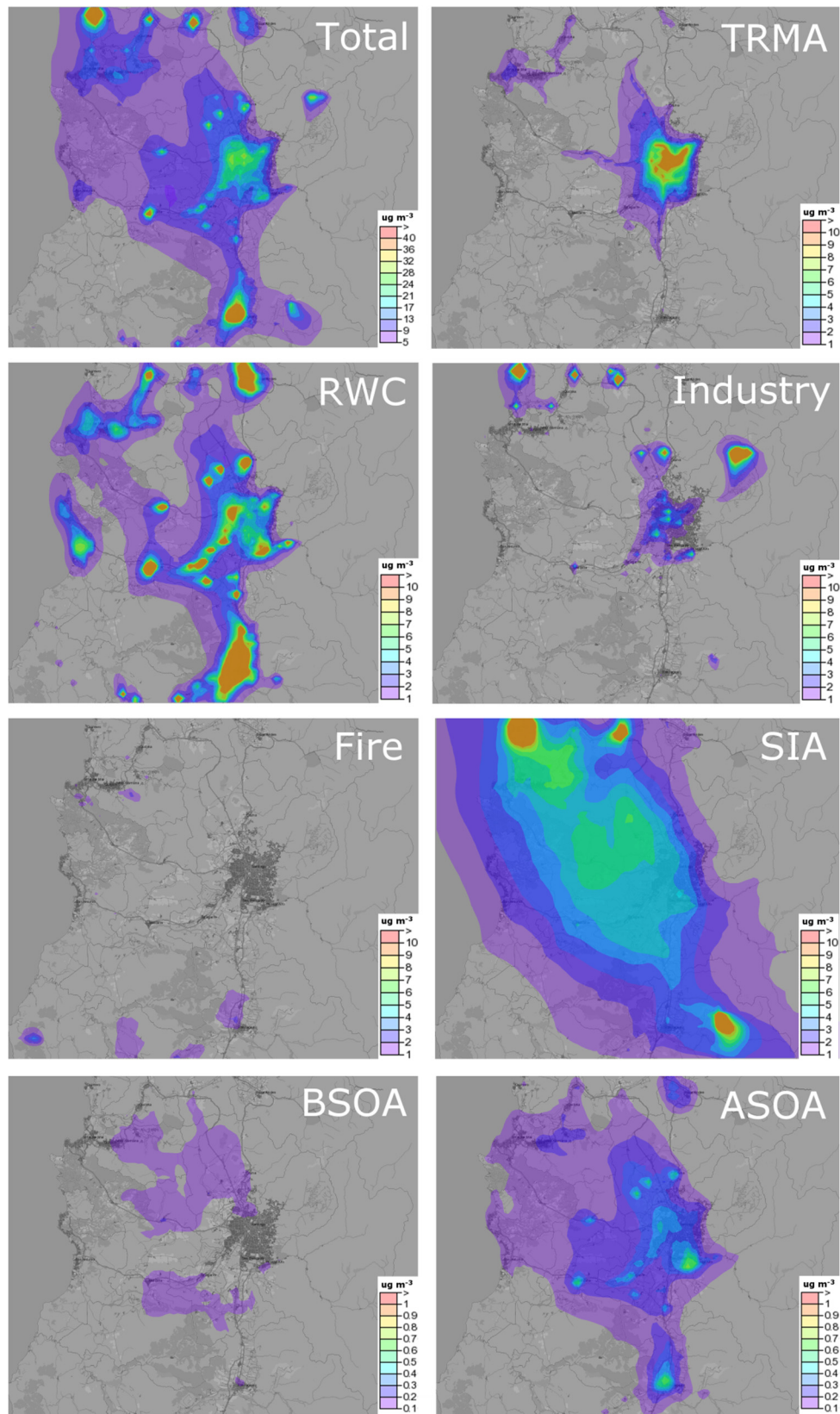
Fig. 12. Simulated total PM$_{2.5}$ for the period 9 March–21 August 2012 (*Total*) and contributions from primary emissions from road transport and machinery (*TRMA*), residential wood combustion (*RWC*), stationary combustion and industrial processes (*Industry*), and wildfires and agricultural burning (*Fire*) as well as secondary inorganic aerosol from all sectors (*SIA*), biogenic secondary organic aerosol (*BSOA*) and anthropogenic secondary organic aerosol from all sectors (*ASOA*). Note that the scale is different for different components. Unit: µg m^{-3}.

agreement between the simulated and the observed concentrations is found for winter than for summer, which possibly results from too slow oxidation of NO_x into HNO_3 in the simulations.

The simulated sector contributions indicate that emissions originating from transport and construction machinery dominate the $PM_{2.5}$ in Santiago; however, residential wood combustion is the primary source in the suburbs of Santiago, and urban areas such as Rancagua, Los Andes, San Antonio and Valparaiso. The highest industrial emissions are located in the vicinity of the Ventanas industrial complex to the northwest or associated with mining activities in the Andes to the northeast of Santiago. Away from urban areas, traffic routes and major industrial sources, SIA is estimated to be the largest component of the aerosol, whereas the simulated SOA only contributes a small fraction.

In order to advance our understanding of the contributions from different sectors and regions to the $PM_{2.5}$ in central Chile, future research should focus on:

- Performing and evaluating model simulations for additional time periods and sites with observed chemical separation of PM concentrations.
- Expanding the monitoring network with additional sites and long-term chemical specification of aerosol components.
- Enhancing the emission inventories. For particulate emissions, a more detailed inventory, including re-suspended dust, and a regionally representative split according to the various components (elemental carbon, organic aerosol, particulate sulfate, dust and other inorganic aerosol) would be useful. To form a more accurate description of secondary organic aerosol, estimates of SVOC, IVOC and other SOA-forming VOC emissions are needed.
- Improving the simulation of low wind speed at night.

ACKNOWLEDGMENTS

DISCLAIMER

The authors declare that they have no conflict of interest.

REFERENCES

Aiken, A.C., Decarlo, P.F., Kroll, J.H., Worsnop, D.R., Huffman, J.A., Docherty, K.S., Ulbrich, I.M., Mohr, C., Kimmel, J.R., Sueper, D., Sun, Y., Zhang, Q., Trimborn, A., Northway, M., Ziemann, P.J., Canagaratna, M.R., Onasch, T.B., Alfarra, M.R., Prevot, A.S.H., Dommen, J., Duplissy, J., Metzger, A., Baltensperger, U. and Jimenez, J.L. (2008). O/C and OM/OC ratios of primary, secondary, and ambient organic aerosols with high resolution time-of-flight aerosol mass spectrometry. *Environ. Sci. Technol.*

42: 4478–4485.

Akagi, S.K., Yokelson, R.J., Wiedinmyer, C., Alvarado, M. J., Reid, J.S., Karl, T., Crounse, J.D. and Wennberg, P. O. (2011). Emission factors for open and domestic biomass burning for use in atmospheric models. *Atmos. Chem. Phys.* 11: 4039–4072.

Ambiosis (2011). Estudio diagnóstico Plan de Gestión atmosférica – Región de Valparaíso, construcción de un inventario de emisiones regional. https://mma.gob.cl/wp-content/uploads/2017/12/InformeFinalEstudioDiagnostic oAtmosfericoValpo.pdf, Last Access: 9 December 2019.

Andersson, C., Bergström, R., Bennet, C., Robertson, L., Thomas, M., Korhonen, H., Lehtinen, K.E.J. and Kokkola, H. (2015). MATCH-SALSA – Multi-scale Atmospheric Transport and CHemistry model coupled to the SALSA aerosol microphysics model – Part 1: Model description and evaluation. *Geosci. Model Dev.* 8: 171–189.

Atkinson, R., Baulch, D.L., Cox, R.A., Crowley, J.N., Hampson, R.F., Hynes, R.G., Jenkin, M.E., Rossi, M.J., Troe, J. and IUPAC Subcommittee (2006). Evaluated kinetic and photochemical data for atmospheric chemistry: Volume II – Gas phase reactions of organic species. *Atmos. Chem. Phys.* 6: 3625–4055.

Barraza, F., Lambert, F., Jorquera, H., Villalobos, A.M. and Gallardo, L. (2017). Temporal evolution of main ambient $PM_{2.5}$ sources in Santiago, Chile, from 1998 to 2012. *Atmos. Chem. Phys.* 17: 10093–10107.

Bergström, R., Denier van der Gon, H.A.C., Prévôt, A.S.H., Yttri, K.E. and Simpson, D. (2012). Modelling of organic aerosols over Europe (2002–2007) using a volatility basis set (VBS) framework: Application of different assumptions regarding the formation of secondary organic aerosol. *Atmos. Chem. Phys.* 12: 8499–8527.

Birch, M. and Cary, R.A. (1996). Elemental carbon-based method for monitoring occupational exposures to particulate diesel exhaust. *Aerosol. Sci. Technol.* 25: 221–241.

Cakmak, S., Dales, R.E. and Vida, C.B. (2009). Components of particulate air pollution and mortality in Chile. *Int. J. Occup. Environ. Health* 15: 152–158.

Carbone, S., Saarikoski, S., Frey, A., Reyes, F., Reyes, P., Castillo, M., Gramsch, E., Oyola, P., Jayne, J., Worsnop, D.R. and Hillamo, R. (2013). Chemical characterization of submicron aerosol particles in Santiago de Chile. *Aerosol Air Qual. Res.* 13: 462–473.

Carter, W.P. (1996). Condensed atmospheric photooxidation mechanisms for isoprene. *Atmos. Environ.* 30: 4275–4290.

Chow, J.C., Watson, J.G., Pritchett, L.C., Pierson, W.R., Frazier, C.A. and Purcell, R.G. (1993). The DRI thermal optical reflectance carbon analysis system – description, evaluation and applications in United-States air-quality studies, *Atmos. Environ.* 27: 1185–1201.

Delgado, R., Hernandez, P. and Mena-Carrasco, M. (2014). Operational implementation and performance evaluation of a PM_{10} and $PM_{2.5}$ model for Santiago de Chile. The World Weather Open Science Conference, Montreal, Canada.

DICTUC (2008). Estudio diagnóstico Plan de Gestión Calidad del Aire VI Región. Informe final. http://cataloga

dor.mma.gob.cl:8080/geonetwork/srv/spa/resources.get?uui
d=95ed1cc5-31bf-43e6-9282-36a2901ae13b&fname=Diag
n%C3%B3stico%20y%20Plan%20de%20Gesti%C3%B
3n%20de%20Calidad%20del%20Aire%20VI%20Regi%
C3%B3n.pdf&access=public, Last Access: 9 December
2019.

DMC (2019). Dirección Meteorológica de Chile - Servicios
Climáticos. https://climatologia.meteochile.gob.cl/applic
ation/anual/aguaCaidaAnual/330021/2012, Last Access:
9 December 9 2019.

Flemming, J., Benedetti, A., Inness, A., Engelen, R.J., Jones,
L., Huijnen, V., Remy, S., Parrington, M., Suttie, M.,
Bozzo, A., Peuch, V.H., Akritidis, D. and Katragkou, E.
(2017). The CAMS interim Reanalysis of Carbon
Monoxide, Ozone and Aerosol for 2003–2015. *Atmos.
Chem. Phys.* 17: 1945–1983.

Gallardo, L., Olivares, G., Langner, J. and Aarhus, B.
(2002). Coastal lows and sulfur air pollution in Central
Chile. *Atmos. Environ.* 36: 3829–3841.

Gallardo, L., Barraza, F., Ceballos, A., Galleguillos, M.,
Huneeus, N., Lambert, F., Ibarra, C., Munizaga, M.,
O'Ryan, R., Osses, M., Tolvett, S., Urquiza, A. and Véliz,
K.D. (2018). Evolution of air quality in Santiago: The role
of mobility and lessons from the science-policy interface.
Elem. Sci. Anth. 6: 38.

Garreaud, R., Rutllant, J. and Fuenzalida, H. (2002). Coastal
lows along the subtropical west coast of South America:
Mean structure and evolution. *Mon. Weather Rev.* 130:
75–88.

Genberg, J., Denier van der Gon, H.A.C., Simpson, D.,
Swietlicki, E., Areskoug, H., Beddows, D., Ceburnis, D.,
Fiebig, M., Hansson, H.C., Harrison, R.M., Jennings, S.
G., Saarikoski, S., Spindler, G., Visschedijk, A.J.H.,
Wiedensohler, A., Yttri, K.E. and Bergström, R. (2013).
Light-absorbing carbon in Europe – measurement and
modelling, with a focus on residential wood combustion
emissions. *Atmos. Chem. Phys.* 13: 8719–8738.

Gidhagen, L., Schmidt-Thomé, P, Kahelin, H. and
Johansson, C. (2002). Anthropogenic and natural levels
of arsenic in PM_{10} in Central and Northern Chile. *Atmos.
Environ.* 36: 3803–3817.

Gramsch, E., Cereceda-Balic, F., Ormeño, I., Palma, G. and
Oyola, P. (2004). Use of the light absorption coefficient to
monitor elemental carbon and $PM_{2.5}$. Example of Santiago
de Chile. *J. Air Waste Manage. Assoc.* 54: 799–808.

Gramsch, E., Cereceda-Balic, F., Oyola, P. and von Baer, D.
(2006). Examination of pollution trends in Santiago de
Chile with cluster analysis of PM_{10} and Ozone data.
Atmos. Environ. 40: 5464–5475.

Gramsch, E., Le Nir, G., Araya, M., Rubio, M.A., Moreno,
F. and Oyola, P. (2013). Influence of large changes in
public transportation (Transantiago) on the black carbon
pollution near streets. *Atmos. Environ.* 65: 153–163.

Gramsch, E., Reyes, F., Vásquez, Y., Oyola, P. And Rubio,
M.A. (2016). Prevalence of Freshly Generated Particles
during Pollution Episodes in Santiago de Chile. *Aerosol
Air Qual. Res.* 16: 2172–2185.

Grass, D. and Cane, M. (2008). The effects of weather and
air pollution on cardiovascular and respiratory mortality

in Santiago, Chile, during the winters of 1988–1996. *Int.
J. Climatol.* 28: 1113–1126.

Grell, G., Peckham, S.E., Schmitz, R., McKeen, S.A., Frost,
G., Skamarock, W.C. and Eder, B. (2005). Fully coupled
"online" chemistry within the WRF model. *Atmos.
Environ.* 39: 6957–6975.

Guenther, A.B., Jiang, X., Heald, C.L., Sakulyanontvittaya,
T., Duhl, T., Emmons, L.K. and Wang, X. (2012). The
Model of Emissions of Gases and Aerosols from Nature
version 2.1 (MEGAN2.1): An extended and updated
framework for modeling biogenic emissions. *Geosci.
Model Dev.* 5: 1471–1492.

Henríquez, A., Osses, A., Gallardo, L. and Resquin, M.D.
(2015). Analysis and optimal design of air quality
monitoring networks using a variational approach. *Tellus
B* 67: 25385.

Kuenen, J.J.P., Visschedijk, A.J.H., Jozwicka, M. and
Denier van der Gon, H.A.C. (2014). TNO-MACC_II
emission inventory; a multi-year (2003–2009) consistent
high-resolution European emission inventory for air
quality modelling. *Atmos. Chem. Phys.* 14: 10963–10976.

Langner, J., Bergström, R. and Pleijel, K. (1998a). European
scale modeling of sulfur, oxidised nitrogen and
photochemical oxidants. Model development and
evaluation for the 1994 growing season. SMHI RMK 82,
SMHI SE-60176 Norrköping, Sweden.

Langner, J., Robertson, L., Persson, C. and Ullerstig A.
(1998b). Validation of the operational emergency response
model at the Swedish Meteorological and Hydrological
Institute using data from ETEX and the Chernobyl
accident. *Atmos. Environ.* 32: 4325–4333.

Mazzeo, A., Huneeus, N., Ordoñez, C., Orfanoz-Cheuquelaf,
C., Menut, L., Mailler, S., Valari, M., Denier van der Gon,
H., Gallardo, L., Muñoz, R., Donoso, R., Galleguillos, M.,
Osses, M. and Tolvett, S. (2018). Impact of residential
combustion and transport emissions on air pollution in
Santiago during winter. *Atmos. Environ.* 190: 195–208.

Mentel, Th.F., Kleist, E., Andres, S., Dal Maso, M., Hohaus,
T., Kiendler-Scharr, A., Rudich, Y., Springer, M., Tillmann,
R., Uerlings, R., Wahner, A. and Wildt, J. (2013). Secondary
aerosol formation from stress-induced biogenic emissions
and possible climate feedbacks. *Atmos. Chem. Phys.* 13:
8755–8770.

Moldanová, J., Bergström, R. and Langner, J. (2002). A
Photolysis Scheme for Photochemical Modelling of the
Troposphere and Lower Stratosphere. Proceedings from
the EUROTRAC-2 Symposium 2002, Midgley, P.M. and
Reuther, M. (Eds.), Margraf Verlag, Weikersheim.

Moreno, F., Gramsch, E., Oyola, P. and Rubio, M.A. (2010).
Modification in the soil and traffic-related sources of
particle matter between 1998 and 2007 in Santiago de
Chile. *J. Air Waste Manage. Assoc.* 60: 1410–1421.

Ng, N.L., Herndon, S.C., Trimborn, A., Canagaratna, M.R.,
Croteau, P.L., Onasch, T.B., Sueper, D., Worsnop, D.R.,
Zhang, Q., Sun, Y.L. and Jayne, J.T. (2011). An aerosol
chemical speciation monitor (ACSM) for routine
monitoring of the composition and mass concentrations
of ambient aerosol. *Aerosol Sci. Technol.* 45: 770–784.

Olivares, G., Gallardo, L., Langner, J. and Aarhus, B.

(2002). Regional dispersion of oxidized sulfur in Central Chile. *Atmos. Environ.* 36: 3819–3828.

Ots, R., Young, D.E., Vieno, M., Xu, L., Dunmore, R.E., Allan, J.D., Coe, H., Williams, L.R., Herndon, S.C., Ng, N.L., Hamilton, J.F., Bergström, R., Di Marco, C., Nemitz, E., Mackenzie, I. A., Kuenen, J.J.P., Green, D. C., Reis, S. and Heal, M.R. (2016). Simulating secondary organic aerosol from missing diesel-related intermediate-volatility organic compound emissions during the Clean Air for London (ClearfLo) campaign. *Atmos. Chem. Phys.* 16: 6453–6473.

Passant, N. (2002). Speciation of UK emissions of non-methane volatile organic compounds, Rep. AEAT/ENV/R/0545, https://uk-air.defra.gov.uk/assets/d ocuments/reports/empire/AEAT_ENV_0545_final_v2.p df, Last Access: 9 December 2019.

Reid, J.S., Koppmann, R., Eck, T.F. and Eleuterio, D.P. (2005). A review of biomass burning emissions part II: Intensive physical properties of biomass burning particles. *Atmos. Chem. Phys.* 5: 799–825.

Robertson, L., Langner, J. and Engardt, M. (1999). An Eulerian limited-area atmospheric transport model. *J. Appl. Meteorol.* 38: 190–210.

Robinson, A.L., Donahue, N.M., Shrivastava, M.K., Weitkamp, E.A., Sage, A.M., Grieshop, A.P., Lane, T.E., Pierce, J.R. and Pandis, S.N. (2007). Rethinking organic aerosols: Semivolatile emissions and photochemical aging. *Science* 315: 1259–1262.

Seinfeld, J.H. and Pandis, S.N. (2016). *Atmospheric chemistry and physics: From air pollution to climate change*, Third edition, John Wiley & Sons, Inc, Hoboken, New Jersey.

Simpson, D., Benedictow, A., Berge, H., Bergström, R., Emberson, L.D., Fagerli, H., Flechard, C.R., Hayman, G.D., Gauss, M., Jonson, J.E., Jenkin, M.E., Nyíri, A., Richter, C., Semeena, V.S., Tsyro, S., Tuovinen, J.P., Valdebenito, Á. and Wind, P. (2012). The EMEP MSC-W chemical transport model – technical description. *Atmos. Chem. Phys.* 12: 7825–7865.

SINCA (2018). Chilean National Air Quality Information System, https://sinca.mma.gob.cl, Last Access: Jannary 2019.

Skamarock, Klemp, W.C., Dudhia, J.B.J., Gill, D.O., Barker, D.M., Duda, M.G., Huang, X.Y., Wang, W. and Powers, J.G. (2008). A description of the advanced research WRF version 3, NCAR Tech. Note NCAR/TN-475+ STR.

Tagle, M., Reyes, F., Vásquez, Y., Carbone, S., Saarikoski, S., Timonen, H., Gramsch, E. and Oyola, P. (2018). Spatiotemporal variation in composition of submicron particles in Santiago Metropolitan Region, Chile. *Front. Environ. Sci.* 6: 27.

Turpin, B.J. and Lim, H.J. (2001). Species contributions to PM$_{2.5}$ mass concentrations: Revisiting common assumptions for estimating organic mass. *Aerosol Sci. Technol.* 35: 602–610.

USACH (2014). Actualización y sistematización del inventario de emisiones de contaminantes atmosféricos en la región metropolitana. Informe final. Departamento de Física, Universidad de Santiago de Chile, Chile.

Villalobos, A.M., Barraza, F., Jorquera, H. and Schauer, J.J. (2015). Chemical speciation and source apportionment of fine particulate matter in Santiago, Chile, 2013. *Sci. Total Environ.* 512–513: 133–142.

Watson, J.G., Chow, J.C. and Chen, L.W.A. (2005). Summary of organic and elemental carbon/black carbon analysis methods and intercomparisons. *Aerosol Air Qual. Res.* 5: 65–102.

Wu, C., Huang, X.H.H., Ng, W.M., Griffith, S.M. and Yu, J.Z. (2016). Inter-comparison of NIOSH and IMPROVE protocols for OC and EC determination: Implications for inter-protocol data conversion, *Atmos. Meas. Tech.* 9: 4547–4560.